

2420 0050

(79A)

Item 50

**Ralph J. Roberts  
CENTER FOR RESEARCH  
IN  
ECONOMIC GEOLOGY**

**ANNUAL RESEARCH  
MEETING-1998**

**Program and Reports**

**7-8 January 1999  
Midby-Byron Building  
Room 107-109  
University of Nevada, Reno  
Reno, NV 89557**

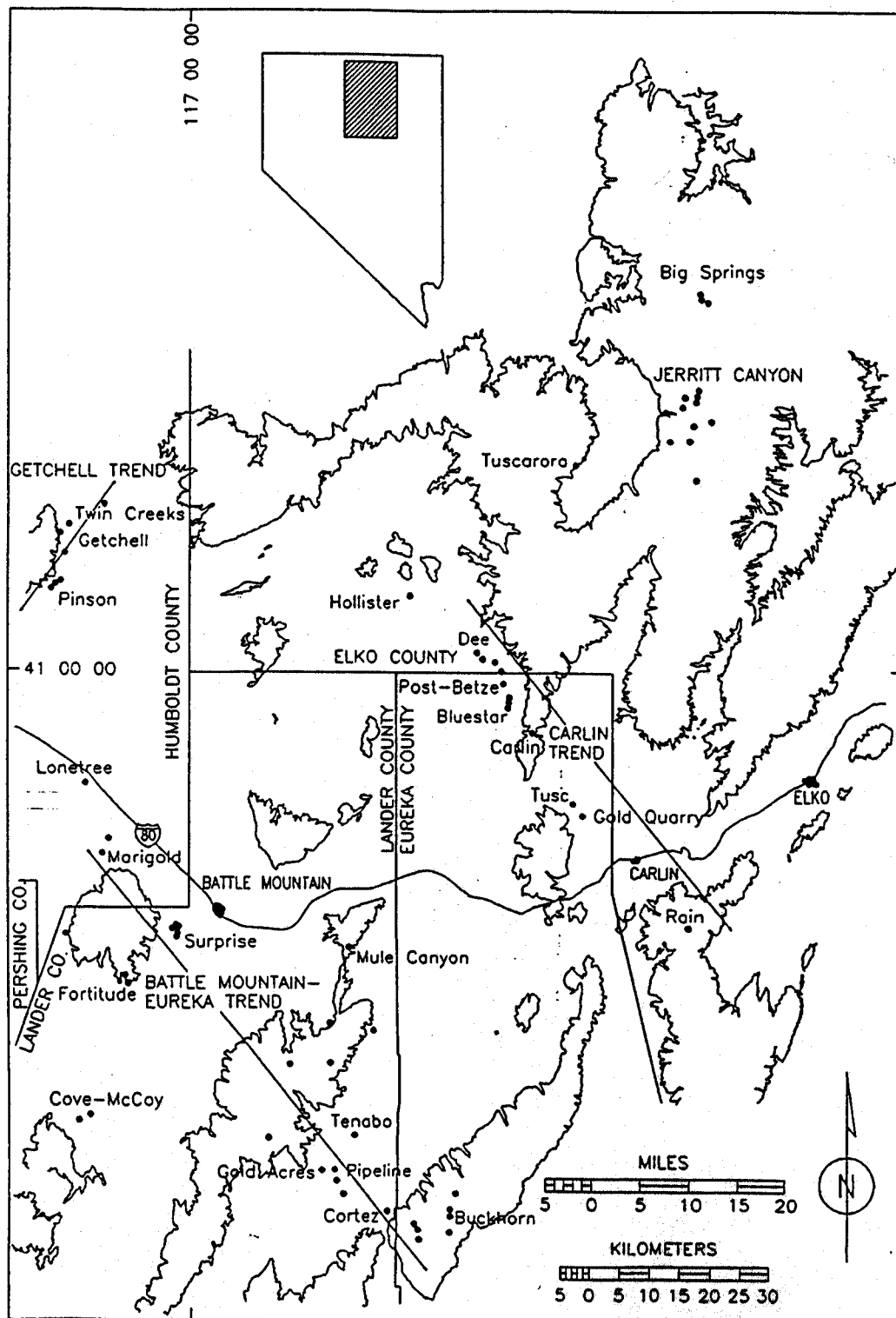


**Figure 1: Location map for the Jerritt Canyon District (adapted from Phinisey, et al., 1996)**

**Geology, Alteration, and Geochemical Dispersion in the  
Paleohydrologic System at the SSX mine, Jerritt Canyon District,  
Elko County, Nevada**

Alex Dewitt

University of Nevada, Reno, Dept. of Geological Sciences

Dr. Tommy Thompson, Faculty Advisor

## **Introduction**

The SSX deposit (South Saval Extension) is one of several sedimentary rock-hosted gold deposits in the Jerritt Canyon District. The district is located in the north-central part of the Independence Mountains, approximately 40 miles north-northwest of Elko, Nevada (fig. 1). The location of the SSX deposit is shown in figure 2, and it was discovered by exploration drilling along structural features observed by geologists in the Saval open-pit. The SSX mine is located 500 to 1000 feet below the surface, and is being mined by underground methods (underhand stope/fill) at an average grade of approximately 0.4 oz/ton with a cutoff of 0.2 oz/ton. The goal of this research is to characterize the ore system in terms of fluid flow paths using alteration/geologic mapping and geochemical data, supported by petrographic and instrumental analyses.

## ***Geologic Units***

The geology of the district is characterized by faulted and folded Paleozoic sedimentary rocks of the lower and upper plates of the Roberts Mountains thrust (Birak, 1986). The upper plate rocks are pelagic, siliciclastic and volcanic rocks of the Upper Cambrian to Middle Ordovician Snow Canyon Formation (Leslie, 1990). The lower plate rocks include portions of the Ordovician Pogonip Group, the Ordovician Eureka Quartzite, the Ordovician-Silurian Hanson Creek Formation, and a Silurian portion of the Roberts Mountains Formation (Hofstra et al., 1991). There are also four distinct types of intrusive rock recognized in the

district: a Pennsylvanian basalt dike and three Tertiary types ranging in composition from basalt to quartz monzonite (Phinisey, 1995).

The units exposed in the SSX mine area are the Hanson Creek Formation, the Roberts Mountains Formation and the Snow Canyon Formation, all of which are intruded by a basalt dike (likely to be one of the Pennsylvanian basalt dikes described by Phinisey). The Hanson Creek Formation has been divided into five distinct units by IMC staff and labeled numerically from top to bottom (order of appearance in surface drilling). The following descriptions are in order from oldest to youngest. Hanson 5 is described as fine-grained, laminated limestone with sparse chert nodules. Hanson 4 is a banded, fine to medium-grained, laminated, thinly bedded limestone with abundant chert nodules. Hanson 3, the primary host for gold mineralization, is a rhythmically interbedded, locally fossiliferous micrite and calcareous siltstone, which grades upward from nodular and undulatory bedding surfaces to tabular and planar beds. Hanson 2 is a fine-grained, locally dolomitic limestone with the least amount of silty particles. Hanson 1 is a unit consisting of tabular, rhythmically interbedded chert, limestone, and dolostone (Hohbach and Roth, 1983). The Saval Discontinuity separates the Hanson Creek Formation from the overlying Roberts Mountains Formation which is best described as a locally carbonaceous, finely laminated calcareous siltstone.

### **Orebody Controls**

There appear to be two primary factors controlling ore-grade gold mineralization at SSX: 1) stratigraphy, and 2) structural controls. The ore is hosted mainly within the Hanson Creek Formation in unit 3, where the enhanced permeability of silty interbeds appears to have conducted fluids. Samples of micritic beds and silty interbeds were collected and assayed by I.M.C. mine geologists. Silty interbeds were found to contain significantly higher gold values than micrite beds. Silty interbeds also exhibit alteration features that will be described in the following section.

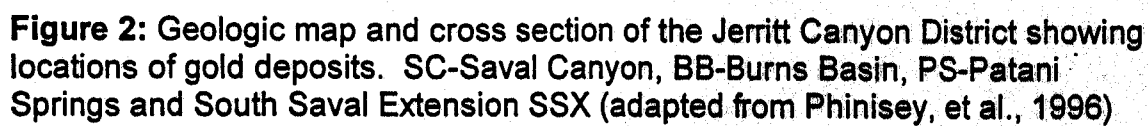


**Figure 2: Geologic map and cross section of the Jerritt Canyon District showing locations of gold deposits. SC-Saval Canyon, BB-Burns Basin, PS-Patani Springs and South Saval Extension SSX (adapted from Phinisey, et al., 1996)**

The second factor controlling ore-grade mineralization is structure. There are two important sets of faults. The older set is partially occupied by the basalt dike (labeled by mine geologists as the South Boundary Fault), and strikes N70W to N50W with nearly vertical dips. These older faults are 6 to 36-inch, gouge-filled shears characterized by high carbon, arsenic and iron sulfides, and silica content. The dike ranges from 10 to 25 feet in thickness and occupies one of the southernmost of these faults.

There are at least two faults in the mapped workings comprising the younger set of structures. One strikes N16E and dips 60 to 80 NW, and the other strikes approximately N40E and dips 62 NW. Both faults truncate the basaltic dike, have normal and possibly left lateral offset, and share similar features: dolomitized wallrocks, carbon enrichment, arsenic and iron sulfides, silicification, and brecciation (both tectonic and decarbonatization/collapse). The ore mineralization/grade is more substantial with proximity to these structures and is highly localized in the Hanson 3 both in the hanging wall (mapped area) and footwall (not exposed).

## **Alteration**

Four different types of wallrock alteration were mapped in the SSX workings: 1) decarbonatized wallrock; 2) arsenic minerals, 3) carbon enrichment, and 4) silicified rock. The degree of decarbonatization was determined using 10% HCl and categorized by amount of effervescence in terms of weak, moderate, and strong. Decarbonatized rock locally exhibits macroscopic dissolution features such as collapse breccias and slump blocks, but the most consistent evidence for decarbonatization is the development of stylolites. The stylolites are 0.01 mm to 0.8mm thick, crenulated structures, consisting of insoluble residue/carbonaceous material, and locally pyrite, arsenic sulfides, and silica (fig. 3). In weakly decarbonatized Hanson 3, stylolite development is concentrated along and adjacent to siltstone interbeds. Stronger decarbonatization results in a higher concentration of stylolites and a resulting decrease in the thickness of micrite beds. Intensely decarbonatized intervals

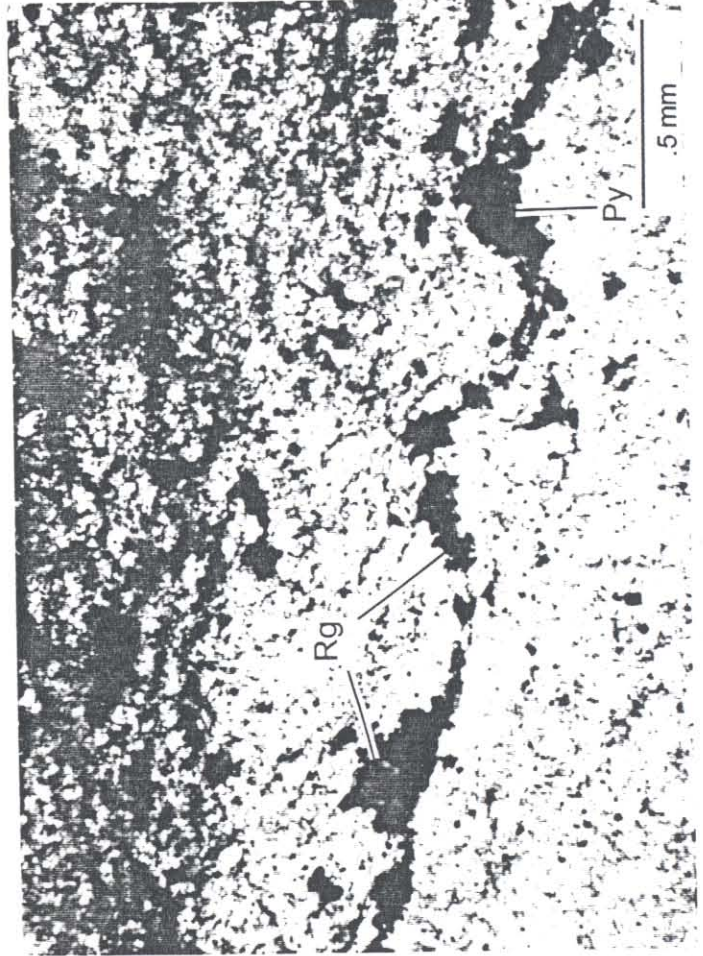




a.



b.



c.

**Figure 3**

- a. Stylolites along siltstone interbeds of Hanson Creek Formation, unit 3, plane light, 40X
- b. Stylolites in fossiliferous Hanson 3 micrite, plane light, 40X
- c. Realgar, pyrite and silica filled stylolite in Hanson 3 micrite, plane light, 100X

without breccia result in a rock with the appearance of equally thick dark and light colored beds. Decarbonatization to the point of sanding is evident in the Hanson 2, and locally in Hanson 3 micrite, although very strongly decarbonatized Hanson 3 results mainly in collapse breccia formation. The strongly decarbonatized rock is localized near structures and is commonly accompanied by other alteration types.

Some of the altered rock that was mapped as decarbonatized is now known to be dolomitized. Petrographic analysis of samples taken near the northeasterly faults revealed rhombic carbonate overgrowths on anhedral "dusty" carbonate grains (fig. 4). Thin-section billets stained with alizarin red indicate dolomite instead of abundant calcite. Dolomitization is localized in northeasterly-trending fault-related breccias. Dolomite is also present in veinlets and as breccia filling between dolomitized fragments.

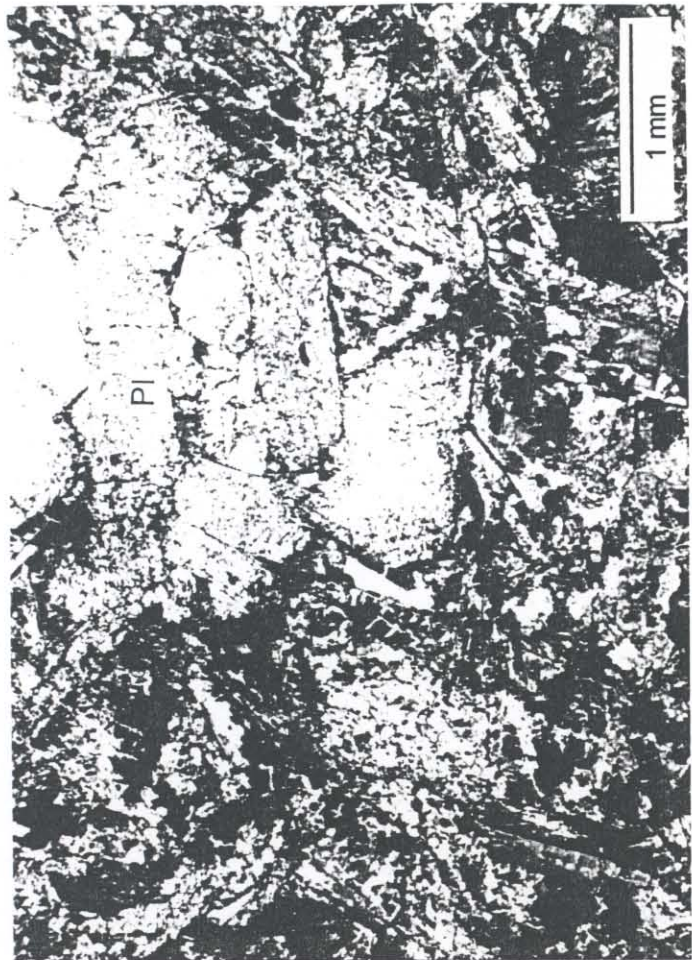
Carbon enrichment is apparent throughout the mapped workings, but is localized in siltstone interbeds adjacent to northeasterly and most northwesterly structures. Outside of the ore zone, carbon flooding is apparent along calcite veins. Arsenic minerals tend to coincide with carbon-enriched rock as well as in silicified rock. Silica is present in veinlets and grains of jigsaw-textured quartz and some chalcedonic quartz veinlets in the basaltic dike, but no true jasperoid was apparent in the mapped area.

Alteration of the basalt dike increases in intensity from east to west approaching the northeasterly faults. The least altered of the dike samples is identical to deuterically altered basaltic dike described by Phinisey (1995) and is characterized by potassium metasomatism resulting in secondary biotite (fig. 5a) and k-feldspar overgrowths on plagioclase (not observed). The next most intense dike-hosted alteration is phyllic alteration characterized by sericite, quartz, pyrite, and leucoxene (fig. 5b). The most intense alteration of the dike is argillic, with abundant kaolinite, sericite, smectite, quartz, carbonate and marcasite (fig. 5c).

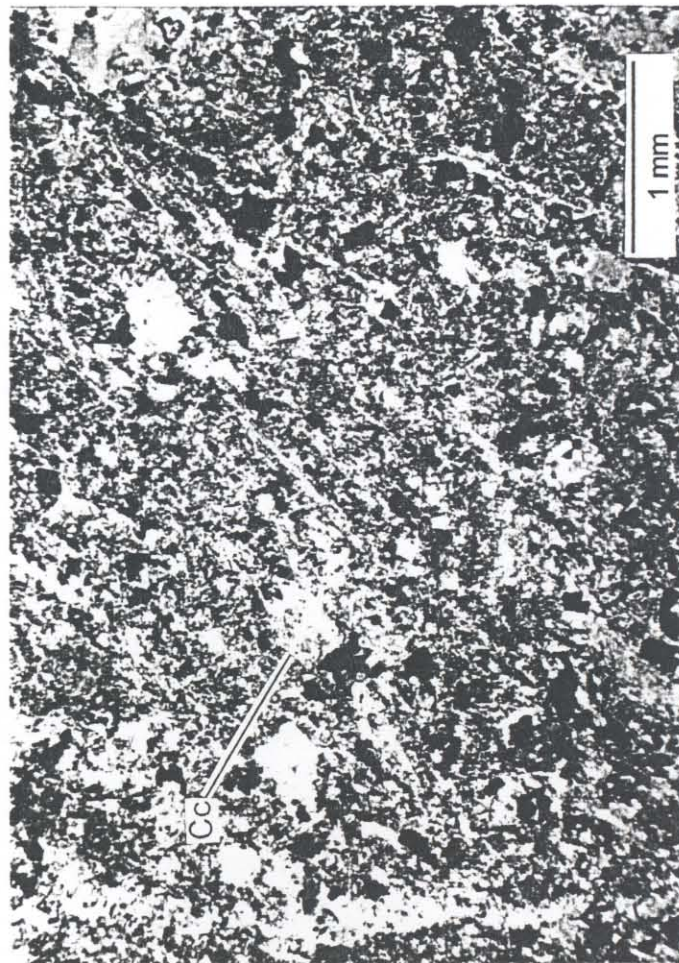




a.



b.



c.

**Figure 5**

- a. Basalt dike with secondary biotite, X-POL, 40X
- b. Basalt dike with sericitized, glomeroporphyritic plagioclase, X-POL, 40X
- c. Basalt dike with argillized plagioclase, abundant sulfides and carbonate, X-POL, 40X

without breccia result in a rock with the appearance of equally thick dark and light colored beds. Decarbonatization to the point of sanding is evident in the Hanson 2, and locally in Hanson 3 micrite, although very strongly decarbonatized Hanson 3 results mainly in collapse breccia formation. The strongly decarbonatized rock is localized near structures and is commonly accompanied by other alteration types.

Some of the altered rock that was mapped as decarbonatized is now known to be dolomitized. Petrographic analysis of samples taken near the northeasterly faults revealed rhombic carbonate overgrowths on anhedral "dusty" carbonate grains (fig. 4). Thin-section billets stained with alizarin red indicate dolomite instead of abundant calcite. Dolomitization is localized in northeasterly-trending fault-related breccias. Dolomite is also present in veinlets and as breccia filling between dolomitized fragments.

Carbon enrichment is apparent throughout the mapped workings, but is localized in siltstone interbeds adjacent to northeasterly and most northwesterly structures. Outside of the ore zone, carbon flooding is apparent along calcite veins. Arsenic minerals tend to coincide with carbon-enriched rock as well as in silicified rock. Silica is present in veinlets and grains of jigsaw-textured quartz and some chalcedonic quartz veinlets in the basaltic dike, but no true jasperoid was apparent in the mapped area.

Alteration of the basalt dike increases in intensity from east to west approaching the northeasterly faults. The least altered of the dike samples is identical to deuterically altered basaltic dike described by Phinisey (1995) and is characterized by potassium metasomatism resulting in secondary biotite (fig. 5a) and k-feldspar overgrowths on plagioclase (not observed). The next most intense dike-hosted alteration is phyllic alteration characterized by sericite, quartz, pyrite, and leucoxene (fig. 5b). The most intense alteration of the dike is argillic, with abundant kaolinite, sericite, smectite, quartz, carbonate and marcasite (fig. 5c).

























## **Paragenetic Relationships**

Petrographic analysis of 80 thin sections and 8 polished-thin sections has permitted a preliminary interpretation of some paragenetic relationships (fig. 6). Early base-metal sulfides present in the basalt dike are replaced by marcasite and arsenic sulfides (fig. 7a). In the arsenic-rich assemblage, a progression from oxidized to more reduced fluids is evidenced by early orpiment replaced and rimmed by realgar (fig. 7b). In the basalt dike, anhedral pyrite is rimmed and replaced by euhedral marcasite, and marcasite veinlets cut earlier realgar (fig. 8).

Away from northeasterly structures and spatially associated arsenic sulfides, arsenopyrite rims on marcasite may represent arsenic mineralization. A backscatter electron image of a rimmed marcasite crystal (fig. 9) reveals a progression from marcasite to arsenopyrite to porous marcasite to arsenical marcasite. This image was taken from a sample of basalt dike in an arsenic sulfide-poor, iron sulfide-rich zone away from a northeasterly fault. Within the ore zone, marcasite is the dominant iron sulfide and realgar is the dominant arsenic sulfide. In the basalt dike, pyrite is rimmed and replaced by marcasite overgrowths. This replacement is progressively more complete with proximity to northeasterly faults, and coincides with more intense alteration of the dike.

Chalcopyrite and sphalerite were found in the basalt dike near northeast-trending faults but outside of the ore zone. Sphalerite commonly has chalcopyrite "disease" and pyrite and marcasite replace these sulfides. Sulfides in the basalt dike are found mainly in ferromagnesian mineral sites and in veinlets. Barite is localized in veinlet cores and breccia vugs.

# *Paragenetic Diagram*

Arsenopyrite			
Arsenical marcasite			
Barite			
Chalcopyrite			
Marcasite	 		
Orpiment			
Pyrite			
Realgar			
Sphalerite	 		
Argillization			
Carbon Enrichment	  		
Decarbonatization	  		
Dolomitization	- ?- -?-		
Phyllic Alteration			
Silicification	  		

**Figure 6**

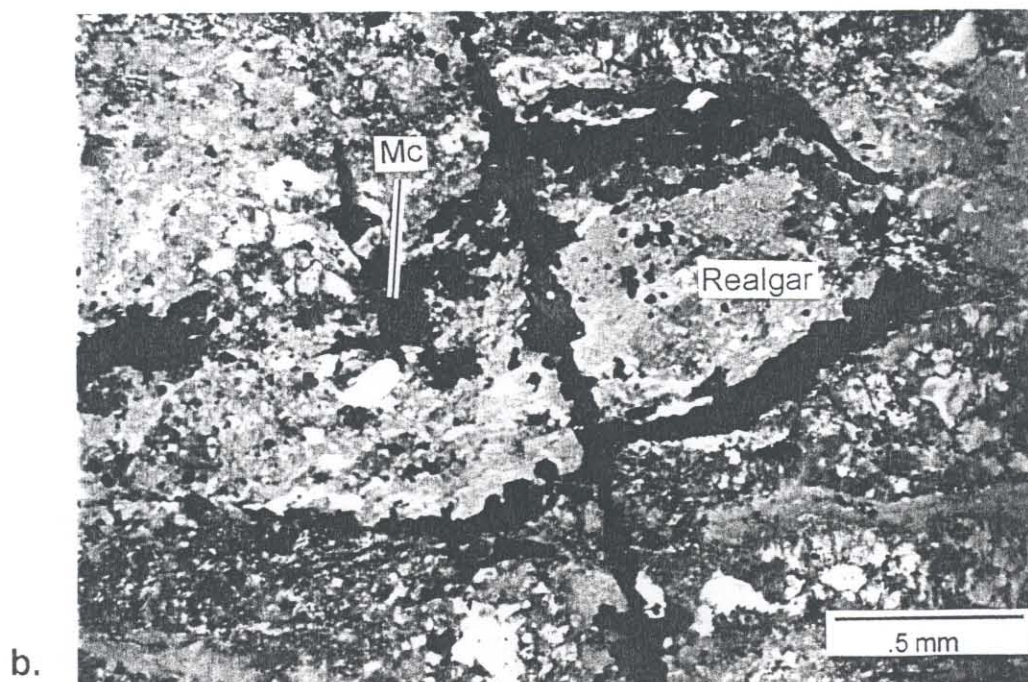
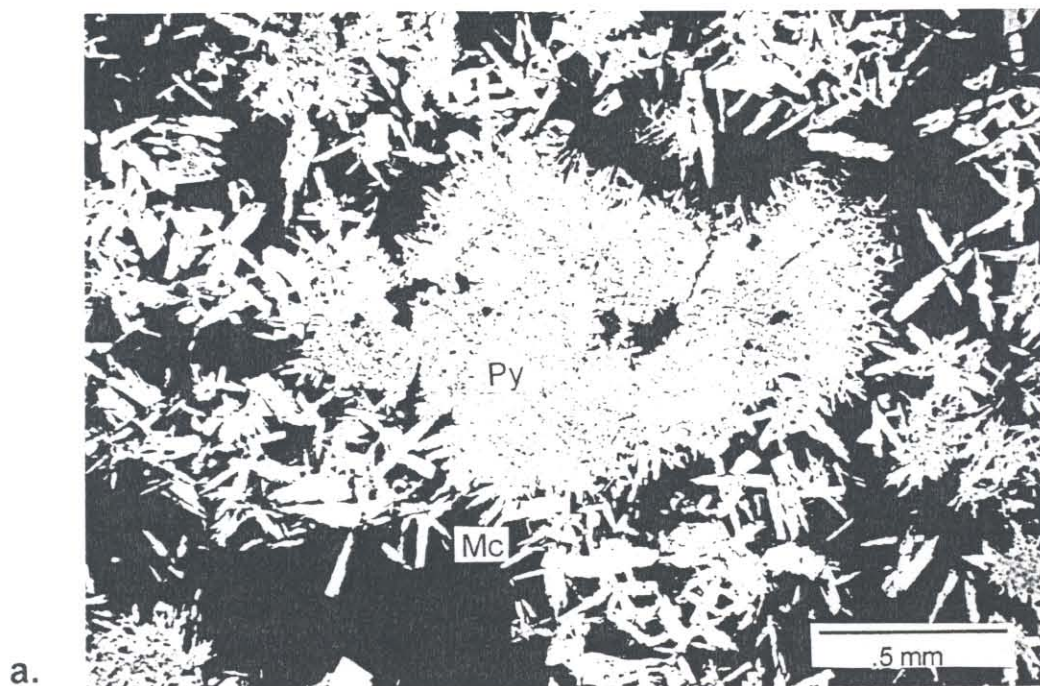


**Figure 8**

- a. Pyrite rimmed by marcasite, reflected light, 100X
- b. Marcasite veinlet cutting realgar, reflected light, X-POL, 100X



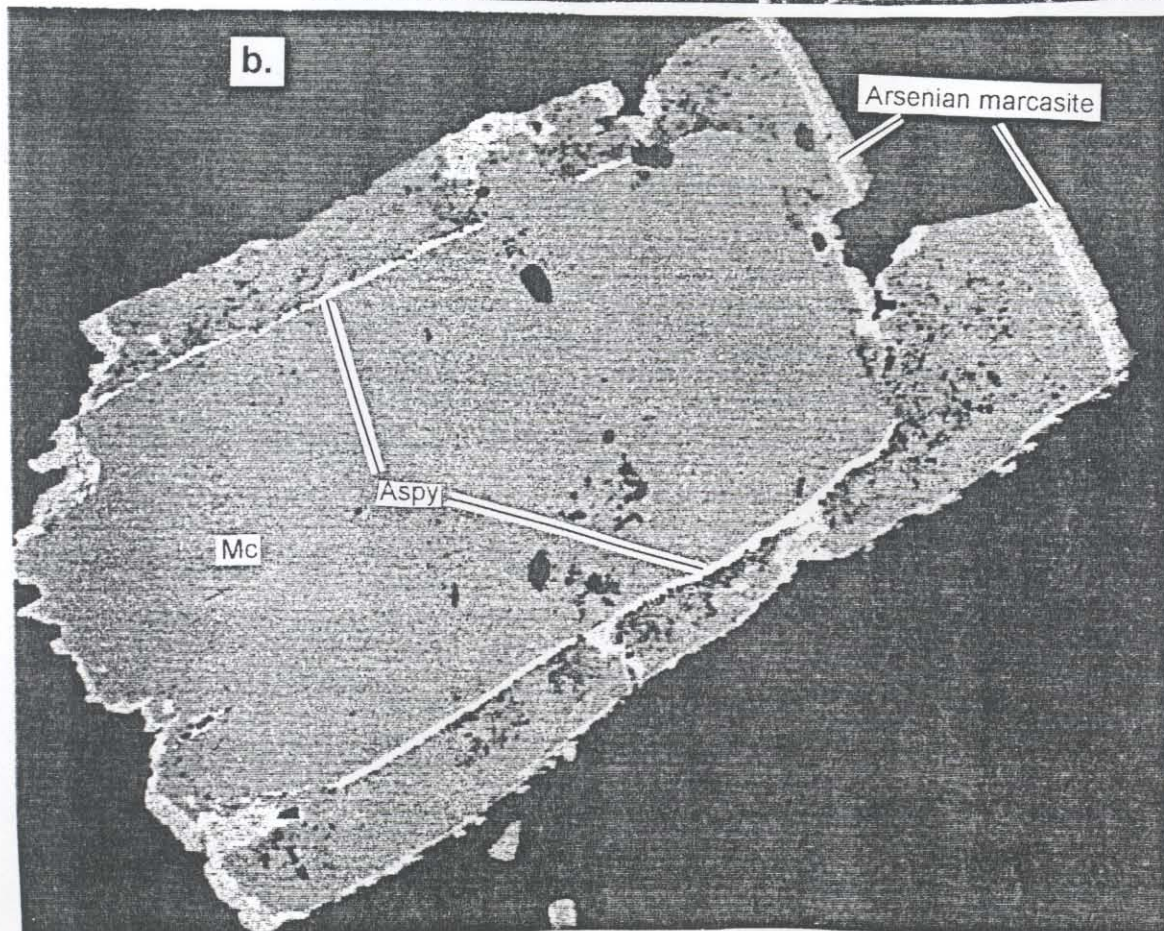
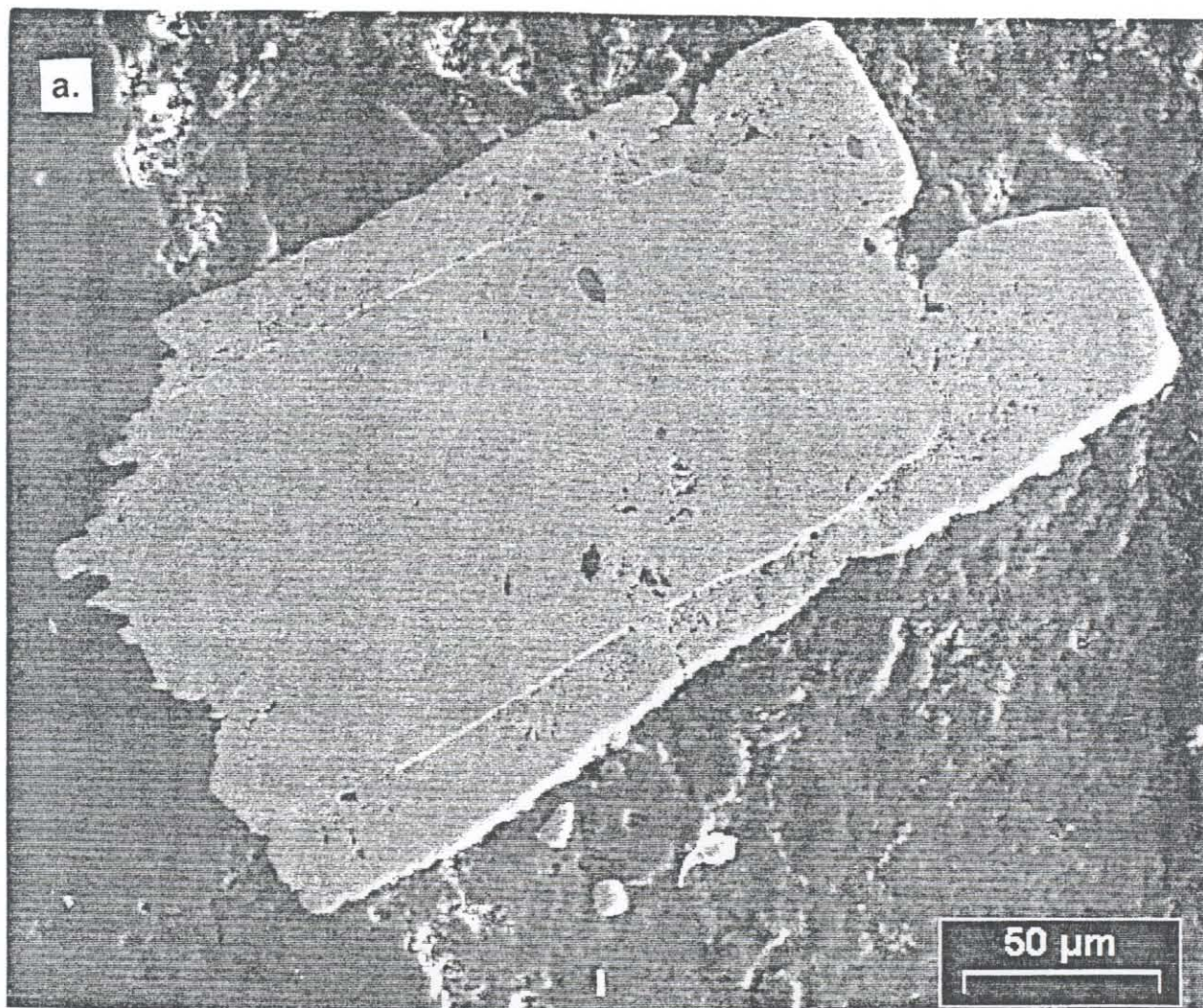


**Figure 9**

- a. Secondary electron image of zoned marcasite, 400X
- b. Backscatter electron Image, 400X



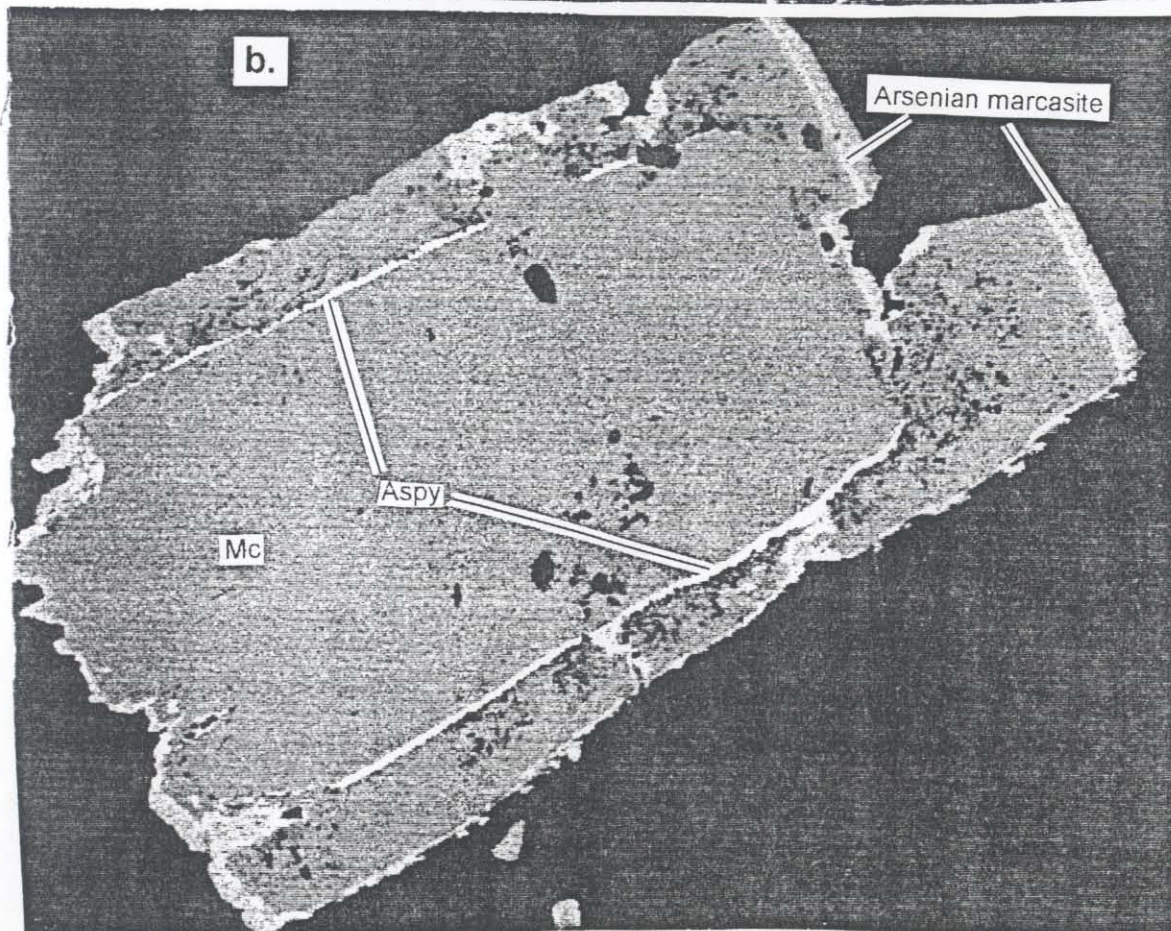
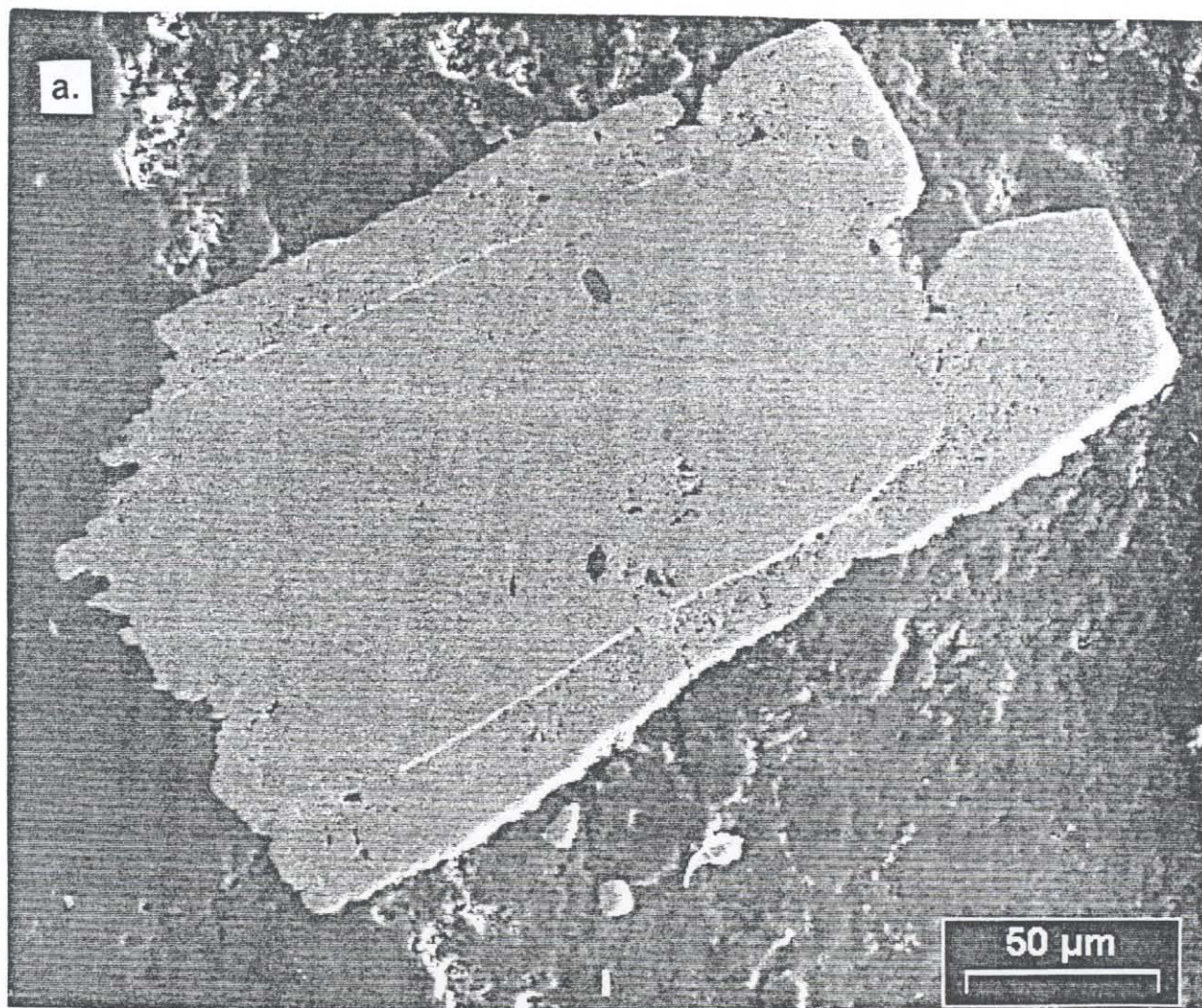


**Figure 9**

a. Secondary electron image of zoned marcasite, 400X

b. Backscatter electron Image, 400X



## **Geochemistry**

The geochemical data for the SSX project area were obtained from 164 surface downhole rotary and core drill-holes covering approximately 1 square mile. The drill-hole depths average approximately 1000 feet and composite samples were taken at average intervals of 50 feet. 3146 samples were analyzed by Chemex Labs for 33 elements: Au (ppb), Ag (ppm), Al (%), As (ppm), Ba (ppm), Be (ppm), Bi (ppm), Ca (%), Cd (ppm), Co (ppm), Cr (ppm), Cu (ppm), Fe (%), Ga (ppm), Hg (ppb), K (%), La (ppm), Mg (%), Mn (ppm), Mo (ppm), Na (%), Ni (ppm), P (ppm), Pb (ppm), Sb (ppm), Sc (ppm), Sr (ppm), Ti (%), Tl (ppm), U (ppm), V (ppm), W (ppm), and Zn (ppm). Of these elements, Be, Bi, Ga, La, Na, Ti, and U were not variable enough for study.

A spreadsheet program was used to organize and analyze the geochemical data. A statistical summary of each element is shown in table 1. A correlation matrix is given in table 2, with significant values (greater than 0.5) in bold. There are six drill-holes within the mapped area that were used to characterize the geochemical profile of major structures.

### *Correlation*

The data were analyzed using a computer and spreadsheet program to generate a correlation matrix (table 2). There are three distinct groups of elements that have a significant correlation. 1) The highest degree of correlation is between cadmium, vanadium and zinc. These elements also have a lesser degree of correlation with silver, molybdenum, nickel, and copper. 2) Scandium, cobalt, iron, aluminum and copper correlate well with each other, and potassium, nickel, chromium and manganese weakly correlate with these elements. 3) Finally, another group of elements that has a significant degree of correlation is gold, mercury, arsenic, and thallium.

Table 1  
Statistical Summary for Downhole Geochemistry,  
SSX Project Area

Element	Mean	Standard Error	Median	Mode	Standard Deviation	Sample Variance	Kurtosis	Skewness	Range	Minimum	Maximum
Au (ppb)	186.6969793	13.65990794	10	0	766.0517293	586835.252	81.42543782	8.128751455	10000	0	10000
Ag (ppm)	0.407408585	0.013105396	0.2	0.1	0.734954556	0.5401582	110.7335725	7.910543447	15.7	0.1	15.8
Al %	0.510864865	0.007560712	0.44	0.45	0.424007015	0.179781949	22.26455153	3.809249708	4.27	0.02	4.29
As (ppm)	92.16947536	6.151963685	24	1	345.0039664	119027.7369	203.7577795	12.35748373	8189	1	8190
Ba (ppm)	426.7230525	6.438755978	350	170	361.0873641	130384.0845	10.81987192	2.629198158	3060	10	3070
Ca %	9.370346582	0.07646663	9.18	15	4.288271497	18.38927243	-0.885936138	-0.236083834	14.85	0.15	15
Cd (ppm)	1.441033386	0.052641837	0.5	0.25	2.952169984	8.715307615	43.95230863	5.829968718	36.75	0.25	37
Co (ppm)	3.88871224	0.087502502	3	3	4.907166518	24.08028324	28.27515863	4.581960924	64.5	0.5	65
Cr (ppm)	78.53481717	1.367946493	57	4	76.71484914	5885.168078	8.291673536	2.433661436	656	0	656
Cu (ppm)	30.07281399	0.502024881	18	6	28.15370574	792.6311468	2.929805855	1.627113965	239	0	239
Fe %	1.129812401	0.013411221	0.96	0.99	0.75210527	0.565662338	12.48492196	2.888084207	7.59	0.09	7.68
Hg (ppb)	2273.045787	129.6693573	340	110	7271.896405	52880477.33	81.30013375	7.840627399	99990	10	100000
K %	0.224798092	0.001898761	0.22	0.21	0.106483069	0.011338644	2.03208005	0.755443397	0.84	0.01	0.85
Mg %	3.462521463	0.03271443	3.83	1.38	1.834635037	3.36588572	-0.406984116	0.177762739	10.32	0.03	10.35
Mn (ppm)	24.26995231	0.351202369	19	16	19.69553406	387.9140619	21.51420584	3.596655988	260	2	262
Mo (ppm)	7.589189189	0.250840171	3	0	14.06719191	197.8858882	19.33749409	3.914505085	125	0	125
Ni (ppm)	31.5036566	0.609276551	21	6	34.16841152	1167.480346	10.36648721	2.827949797	269	1	270
P (ppm)	1276.220986	20.90053046	1000	280	1172.108009	1373837.186	12.4283097	2.762607355	10000	0	10000
Pb (ppm)	6.644833068	0.171422578	6	6	9.61342954	92.41802752	657.9602428	20.91320354	343	1	344
Sb (ppm)	22.31707472	1.887240383	2.6	1.8	105.837006	11201.47184	62.84281496	7.715552863	999.9	0.1	1000
Sc (ppm)	2.568839428	0.050488764	2	2	2.83142502	8.016967641	25.03946068	4.484313995	30	0	30
Sr (ppm)	260.0944356	5.925467857	112	95	332.3020125	110424.6275	2.871438229	2.000156731	1600	0	1600
Tl (ppm)	5.289348172	0.077921407	5	5	4.369855869	19.09564032	1563.651122	35.51905834	205	5	210
V (ppm)	83.98314785	3.906315281	34	3	219.0673312	47990.49558	59.60932696	7.003627511	2749	1	2750
W (ppm)	5.73608903	0.116226302	5	5	6.518005837	42.48440009	688.8647622	24.27947159	225	5	230
Zn (ppm)	143.4015898	4.326822394	86	24	242.649496	58878.77792	40.97561781	5.632716953	2998	2	3000

Table 2  
Correlation Matrix:  
SSX Project Area

	Au	Ag	Al	As	Ba	Ca	Cd	Co	Cr	Cu	Fe	Hg	K	Mg	Mn	Mo	Ni	P	Pb	Sb	Sc	Sr	Tl	V	W	Zn
Au (ppb)	1																									
Ag (ppm)	0.254	1																								
Al %	-0.11	0.036	1																							
As (ppm)	0.639	0.074	-0.02	1																						
Ba (ppm)	-0.04	-0.13	-0	-0.05	1																					
Ca %	0.047	-0.14	-0.51	0.074	0.021	1																				
Cd (ppm)	-0.03	0.532	0.068	0.011	-0.12	0.016	1																			
Co (ppm)	-0.01	-0.01	0.749	0.18	-0.09	-0.43	-0.02	1																		
Cr (ppm)	0.05	0.284	0.269	0.002	-0.03	-0.7	0.122	0.286	1																	
Cu (ppm)	-0.07	0.369	0.53	-0.01	-0.18	-0.57	0.475	0.503	0.445	1																
Fe %	-0.02	0.035	0.812	0.115	-0.11	-0.6	0.015	0.89	0.355	0.647	1															
Hg (ppb)	0.722	0.242	-0.12	0.613	-0.06	0.052	-0.02	0.005	0.085	-0.09	-0.02	1														
K %	-0.13	0.05	0.675	-0.03	-0.12	-0.53	0.088	0.404	0.142	0.498	0.547	-0.14	1													
Mg %	-0.13	-0.02	-0.02	-0.13	0.168	0.182	0.2	-0.14	-0.31	-0.13	-0.12	-0.19	-0.02	1												
Mn (ppm)	-0.07	-0.1	0.426	-0.01	-0	-0.37	-0.09	0.525	0.253	0.371	0.601	-0.11	0.249	-0.1	1											
Mo (ppm)	-0.07	0.445	0.034	-0.05	-0.12	-0.03	0.83	-0.01	0.189	0.496	0.036	-0.06	0.022	0.243	-0.1	1										
Ni (ppm)	-0.08	0.432	0.441	0.043	-0.15	-0.24	0.763	0.466	0.276	0.705	0.47	-0.07	0.276	0.184	0.142	0.8	1									
P (ppm)	-0.04	0.417	0.136	-0.03	-0.1	-0.08	0.431	0.009	0.175	0.42	0.07	-0	0.168	0.144	-0.13	0.393	0.486	1								
Pb (ppm)	-0.05	0.031	0.125	-0.05	0.033	-0.25	0.024	0.114	0.161	0.268	0.189	-0.04	0.142	-0.06	0.213	0.041	0.086	0.042	1							
Sb (ppm)	0.216	0.185	-0.12	0.153	0.007	5E-04	-0.02	-0.07	0.15	-0.08	-0.08	0.329	-0.17	-0.16	-0.11	0.005	-0.06	0.03	-0.04	1						
Sc (ppm)	-0.06	0.012	0.796	0.123	-0.06	-0.32	0.094	0.884	0.171	0.463	0.846	-0.06	0.413	0.075	0.426	0.101	0.539	0.085	0.08	-0.1	1					
Sr (ppm)	0.04	-0.12	-0.33	0.056	-0.15	0.667	-0.12	-0.21	-0.42	-0.36	-0.36	0.04	-0.33	-0.41	-0.17	-0.17	-0.29	-0.22	-0.17	0.003	-0.25	1				
Tl (ppm)	0.566	0.181	-0.03	0.443	-0.05	0.005	4E-04	0.019	0.013	0.039	0.054	0.503	-0.05	-0.03	-0.01	-0.01	-0	-0.02	-0.02	0.183	-0	-0	1			
V (ppm)	-0.07	0.515	0.128	-0.04	-0.1	0.015	0.945	0.022	0.131	0.491	0.047	-0.06	0.099	0.188	-0.06	0.926	0.779	0.427	0.021	-0.02	0.143	-0.11	-0.01	1		
W (ppm)	0.1	-0.02	-0.01	0.13	-0.03	0.039	0.008	0.12	0.024	-0	0.035	0.041	-0.03	-0.05	0.012	0.002	0.024	-0.03	-0.03	0.008	0.076	0.062	0.012	0.007	1	
Zn (ppm)	-0.07	0.504	0.129	-0.05	-0.14	-0.07	0.957	0.05	0.164	0.652	0.039	-0.07	0.135	0.181	-0.01	0.863	0.823	0.437	0.056	-0.03	0.144	-0.17	-0.02	0.947	-0	1
	Au	Ag	Al	As	Ba	Ca	Cd	Co	Cr	Cu	Fe	Hg	K	Mg	Mn	Mo	Ni	P	Pb	Sb	Sc	Sr	Tl	V	W	Zn



### *Relationships to Geology*

The correlation of certain elements is most likely related to lithology. Most notably, Sc, Co, Fe, Al, and Cu ( $\pm$  K, Ni, Cr, Mn) are most elevated in dike samples (Appendix 1). Other elements seem to be associated with structural features. Higher values of Zn, V, Cd and other base metals generally occur in the Roberts Mountains Formation and Snow Canyon Formation above the ore deposit, but high Zn and V values also coincide with northeasterly structures (fig. 10). The observed relationship between early base-metal sulfides and later marcasite may indicate a remobilization of Zn and other elements, with redeposition above the ore deposit along structures and within sedimentary rocks. The geochemical profiles of two drill holes show a typical relationship between Au and As within the ore zone (fig. 11).

### *Flow Paths*

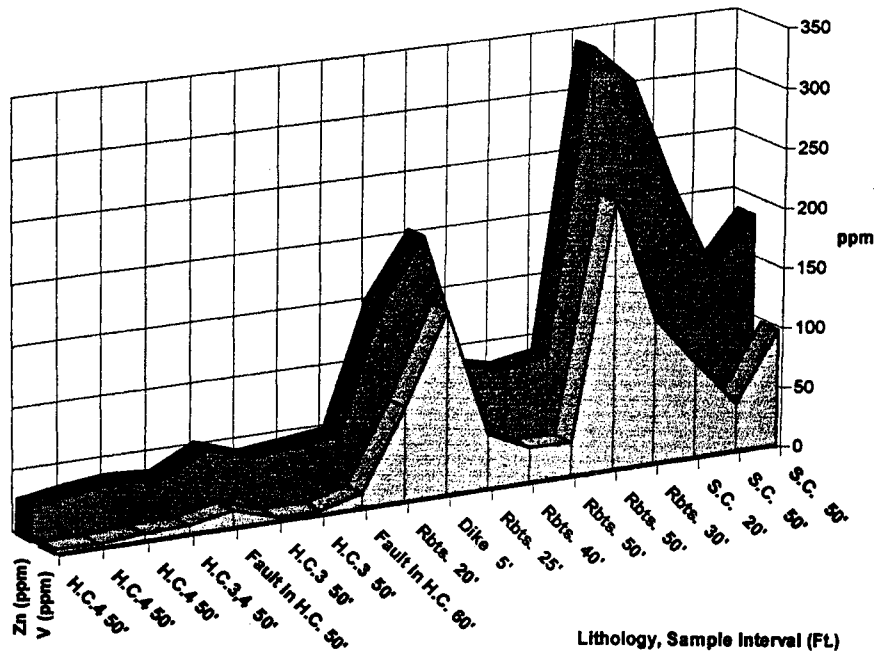
The direction of alteration intensity combined with drill-hole geochemistry may indicate direction of fluid flow. Specific drill-hole intervals were compared at the 7040' level to see if differences could be found with distance from northeasterly structures. The concentrations of Au, As, and Hg steadily increase with proximity to the northeast-trending faults (fig. 12). There is also a decrease in Ca and an increase in Mg toward the faults, as well as a depletion in Al concentration.

### **Discussion**

So far, there is some evidence to suggest that hydrothermal fluids were transmitted primarily along northeast-trending faults. The best indication of this is the fact that ore zones and gold grades increase significantly with proximity to these faults. The older northwest-trending faults also have high grades, but the extent of the ore is much more constrained. Alteration effects are more prominent along the northeast-trending faults, and alteration intensity in the basalt dike increases with proximity to them. On a larger scale, ore grade-

Figure 10

SP-265 Zn, V



SP-339C Zn, V

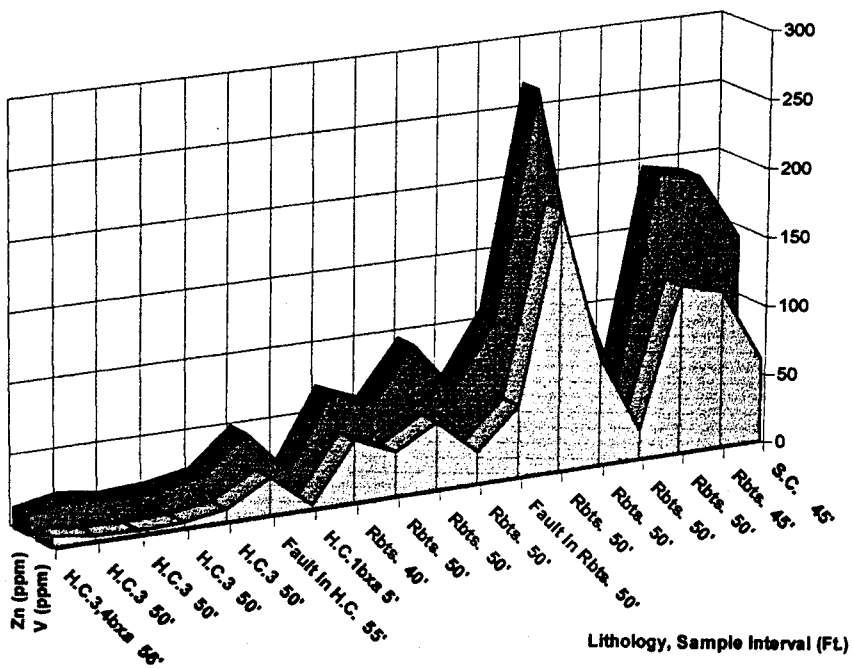
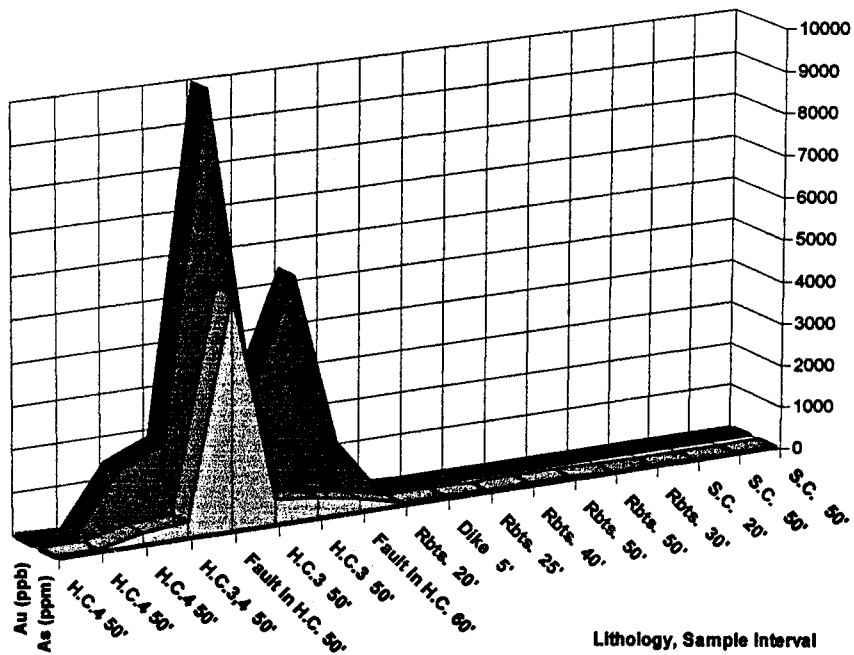


Figure 11

SP-265 Au, As



SP-339C Au, As

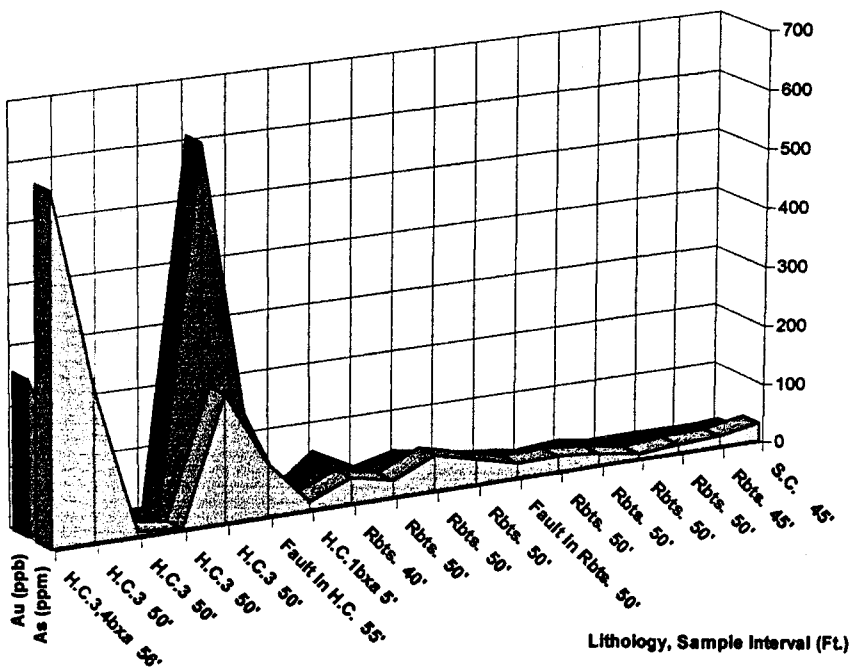
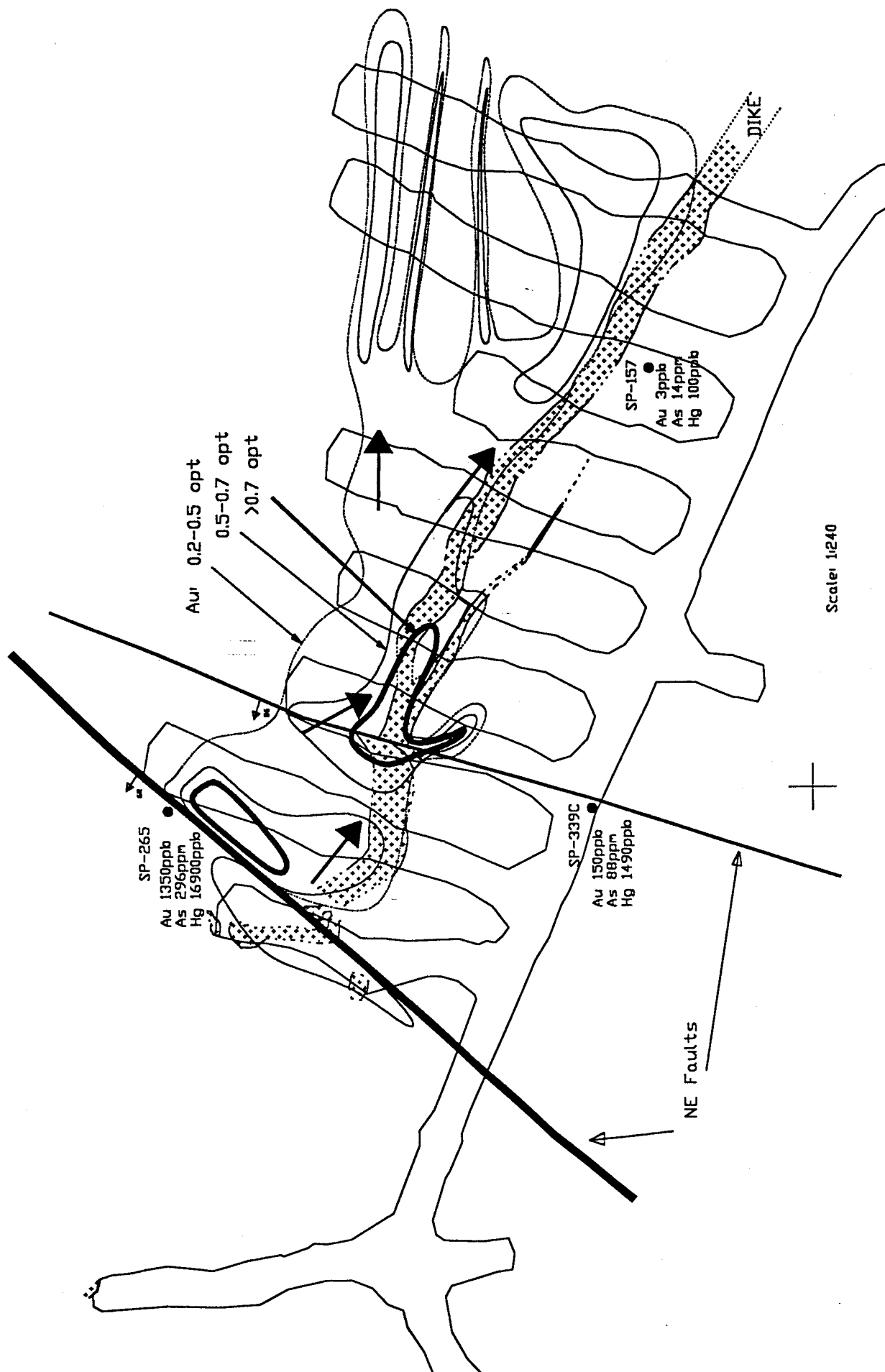


Figure 12  
SSX-7040' level  
Fluid Flow Map



thickness maps for the SSX project area show elongate, northeast-trending ore pods that may lie along these structures where they cut favorable stratigraphy.

The hydrothermal fluids were acidic, as evidenced by the widespread occurrence of marcasite in the ore zone. Paragenetic relationships suggest a fluid that evolved from a relatively oxidized to a more reduced and acidic fluid. Correlation of certain elements may imply that the composition of the ore fluid was enriched in As, Hg, and possibly Tl. Also, the ore fluid was probably siliceous, as petrographic analyses indicate a close relationship between arsenic minerals and silica.

The conspicuous concentration of base-metals in the rocks overlying the ore deposit and adjacent to the northeast-trending faults may indicate remobilization and precipitation of these elements higher up in the hydrothermal plume. The presence of chalcopyrite and sphalerite outside of the ore zone in the basalt dike and observed replacement of these by later iron sulfides may support this idea.

### **Acknowledgments**

Field and petrographic work by Dewitt was supported by funds from the Ralph J. Roberts Center for Research in Economic Geology and the Society of Economic Geologists. The SEG Student Research Grant provided essential funds for travel expenses. The help of Independence Mining Co. geologists and staff is gratefully acknowledged.



### References Cited

- Birak, D. J., 1986, Exploration and geologic development of the Jerritt Canyon gold deposits, Elko County, Nevada, USA, *in*: Gold '86; an international symposium on the geology of gold deposits; proceedings volume. Macdonald, A. J. (editor), GOLD '86. Toronto, ON, Canada. 1986. p. 488-496.
- Hofstra, A. H., Daly, W. E., Birak, D. J., Doe, T. C., 1991, Geologic framework and genesis of Carlin-type gold deposits in the Jerritt Canyon District, Nevada, USA, *in*: Brazil gold '91; the economics, geology, geochemistry and genesis of gold deposits; proceedings. Ladeira, E. A. (editor), A. A. Balkema. Rotterdam, Netherlands. 1991. p. 77-87.
- Hohbach, P and Roth, S, 1983, California Mountain Measured Section, Inter-Office Letter, Independence Mining Co.
- Leslie, S. A., 1990, The Late Cambrian-Middle Ordovician Snow Canyon Formation of the Valmy Group, northeastern Nevada: M. S. thesis, Univ. of Idaho, 112 p.
- Phinisey, J. D., 1995, Petrography, alteration, and mineralization of igneous dikes of the Jerritt Canyon District, Elko County, Nevada: M. S. thesis, Univ. of Nevada, Mackay School of Mines. Reno, NV, 173 p.
- Phinisey, J. D., Hofstra, A. H., Snee, L. W., Roberts, T. T., Dahl, R. J., and Loranger, R. J., 1996, Evidence for multiple episodes of igneous and hydrothermal activity and constraints on the timing of gold mineralization, Jerritt Canyon District, Elko County, Nevada, *in*: Coyner, A. R. and Fahey, P. L., eds., Geology and Ore Deposits of the American Cordillera: Geological Society of Nevada Symposium Proceedings, Reno/Sparks, Nevada, April 1995, Vol. I, p.15-39

Appendix 1:  
SSX Geochemical Data For Surface Drill Holes Intercepting Mapped Workings

SP-362	From	To	Lithology	Au (g/t)	Ag (g/t)	Al %	As (g/t)	Ba (g/t)	Ca %	Cd (g/t)	Co (g/t)	Cr (g/t)	Cu (g/t)	Fe %	Hg (g/t)	K %	Mg %	Mn (g/t)	Mo (g/t)	Ni (g/t)	P (g/t)	Pb (g/t)	Sb (g/t)	Se (g/t)	Sr (g/t)	Ti (g/t)	V (g/t)	W (g/t)	Zn (g/t)	
SP-362	0	50	S.C. 50'	16	0.4	0.57	18	210	0.95	1	7	134	70	1.58	380	0.26	0.51	89	11	42	510	14	1.8	2	61	5	37	5	122	
SP-362	50	100	S.C. 50'	5	0.4	0.57	18	60	2.48	1	7	185	61	1.59	250	0.3	1.29	45	8	36	1380	8	1.2	2	72	5	42	5	154	
SP-362	100	160	S.C. 60'	5	0.2	0.74	48	120	2.07	0.5	6	167	44	1.99	180	0.41	1.25	29	4	32	850	18	1.2	3	50	5	24	5	108	
SP-362	160	200	RHs 40'	3	0.4	0.49	30	190	0.75	2.5	1	68	30	1.22	310	0.24	0.52	25	13	42	1780	8	1.8	3	115	5	82	5	230	
SP-362	200	250	RHs 50'	6	0.1	0.45	34	550	7.87	0.25	1	52	15	0.91	130	0.22	0.41	17	1	19	530	2	0.8	3	77	5	15	5	72	
SP-362	250	300	RHs 50'	2	0.1	0.45	14	410	10.55	0.5	0.5	33	11	0.81	80	0.22	0.59	20	3	18	890	4	1	2	82	5	31	5	64	
SP-362	300	350	RHs 50'	2	0.2	0.5	14	480	10.75	0.5	1	32	21	1	70	0.27	0.57	16	4	28	1140	8	1	3	105	5	26	5	90	
SP-362	350	400	RHs 50'	1	0.2	0.49	12	400	10.25	0.5	2	38	25	1.07	60	0.37	0.84	14	8	33	1090	6	2	3	118	5	41	5	140	
SP-362	400	450	RHs 50'	2	1.4	0.53	44	130	11.1	12.5	3	67	67	1.28	420	0.28	0.52	18	60	143	2750	8	18.5	4	168	5	739	5	100.5	
SP-362	450	500	RHs 50'	12	0.2	0.43	54	290	8.83	2	2	49	22	1.01	280	0.22	0.461	22	10	35	730	6	2.0	3	91	5	92	5	178	
SP-362	500	550	RHs 50'	13	0.1	0.54	28	980	9.9	1	1	41	13	0.95	150	0.29	0.512	23	3	20	780	8	1.4	3	95	5	40	5	96	
SP-362	550	600	RHs 50'	51	0.2	0.95	58	960	8.61	0.5	2	46	11	1	380	0.35	0.44	18	2	17	890	10	1	3	87	5	28	5	64	
SP-362	600	680	RHs 80'	169	0.4	0.84	178	340	8.83	2	1	52	18	1.04	3150	0.32	0.54	23	3	25	1390	12	3	3	69	5	57	5	120	
SP-362	680	715	H.C. 1 20'	715	0.4	0.27	330	250	1.96	1	2	217	12	0.77	9500	0.13	0.79	6	13	26	2690	10	8.8	0	20	5	39	5	86	
SP-362	715	750	H.C. 2.3 50'	3190	0.1	0.14	232	190	15	0.25	0.5	21	8	0.68	1500	0.08	0.57	32	1	7	270	14	12	2	311	5	4	5	28	
SP-362	750	800	Fault in H.C. 3 50'	3520	0.1	0.28	520	190	15	0.5	4	4	18	0.93	37000	0.2	1.3	23	0	6	270	10	5.2	2	675	5	4	5	24	
SP-362	800	860	H.C. 3 60'	6160	0.1	0.3	2140	260	15	1.5	4	9	21	0.84	34900	0.2	1.12	20	0	9	370	8	30	2	649	5	6	5	24	
SP-362C	From	To	Lithology	Au (g/t)	Ag (g/t)	Al %	As (g/t)	Ba (g/t)	Ca %	Cd (g/t)	Co (g/t)	Cr (g/t)	Cu (g/t)	Fe %	Hg (g/t)	K %	Mg %	Mn (g/t)	Mo (g/t)	Ni (g/t)	P (g/t)	Pb (g/t)	Sb (g/t)	Se (g/t)	Sr (g/t)	Ti (g/t)	V (g/t)	W (g/t)	Zn (g/t)	
SP-362C	500	560	RHs 80'	3580	2.4	0.03	168	770	0.25	0.25	1.5	4	70	18	0.91	3150	0.3	0.423	15	1	23	1980	1	5.8	2	77	5	61	5	120
SP-362C	560	587	H.C. 1 20'	3580	2.4	0.03	198	770	0.25	0.25	2	415	13	0.54	33200	0.01	0.03	3	6	12	630	2	20	0	6	5	5	5	32	
SP-362C	587	647	H.C. 2.3 60'	994	0.8	0.44	462	470	15	0.25	4	48	14	0.9	9600	0.21	0.424	23	1	14	370	2	12	4	559	5	18	10	28	
SP-362C	647	652	Dike 3'	11	0.1	2.74	5340	280	10.1	0.25	300	180	64	0.28	18800	0.55	2.97	60	0	107	970	4	32	21	426	5	108	20	44	
SP-362C	652	662	H.C. 3 10'	11	0.1	0.46	560	490	15	0.25	7	47	16	1.05	2100	0.2	1.49	35	0	25	270	1	4.8	5	1000	3	21	10	22	
SP-362C	662	717	Dike 55'	30	0.1	2.15	1890	210	7.09	0.25	330	175	67	5.18	7450	0.41	3.28	73	0	131	1090	1	12.5	22	248	5	100	20	46	
SP-362C	717	752	H.C. 3 35'	5160	0.1	0.35	1420	60	15	0.25	6	21	12	1.08	12600	0.18	0.86	35	0	13	250	2	4.0	4	895	5	12	230	24	
SP-362C	752	802	H.C. 3 50'	4270	0.1	0.29	972	130	15	0.25	2	18	8	0.81	9050	0.2	1.39	26	0	8	210	4	2	2	1160	5	6	30	18	
SP-362C	802	852	H.C. 3 50'	578	0.1	0.19	138	100	15	0.25	2	17	5	0.51	1100	0.13	1.28	19	0	5	190	2	0	1	1365	5	7	10	14	
SP-362C	852	903	H.C. 3 51'	52	0.1	0.15	138	210	15	0.25	2	14	6	0.55	4150	0.12	0.99	20	0	7	230	2	12.5	1	1145	5	7	10	16	
SP-362C	903	953	H.C. 4 47'	31	0.8	0.14	334	320	15	0.25	2	59	6	0.44	14800	0.08	2.79	15	3	21	2540	1	80	1	152	5	10	20	20	
SP-362C	953	1000	H.C. 4 47'	2	0.1	0.07	30	40	15	0.25	1	22	1	0.14	2950	0.03	1.77	8	0	3	1620	2	11.5	0	370	5	6	10	20	
SP-157	From	To	Lithology	Au (g/t)	Ag (g/t)	Al %	As (g/t)	Ba (g/t)	Ca %	Cd (g/t)	Co (g/t)	Cr (g/t)	Cu (g/t)	Fe %	Hg (g/t)	K %	Mg %	Mn (g/t)	Mo (g/t)	Ni (g/t)	P (g/t)	Pb (g/t)	Sb (g/t)	Se (g/t)	Sr (g/t)	Ti (g/t)	V (g/t)	W (g/t)	Zn (g/t)	
SP-157	0	50	S.C. 50'	10	0.4	0.95	12	520	5.43	2.5	6	123	62	1.61	310	0.24	2.53	61	10	32	950	20	3.4	3	78	5	108	5	270	
SP-157	50	100	S.C. 50'	5	0.1	0.96	4	620	5.4	0.5	4	99	40	1.4	180	0.29	0.521	34	2	17	840	14	1.4	2	104	5	22	5	74	
SP-157	100	150	S.C. 50'	8	0.8	0.56	6	240	4.16	0.5	6	165	44	1.41	180	0.26	2.36	47	11	32	480	8	1.4	2	109	5	30	5	102	
SP-157	150	200	S.C. 50'	11	0.8	0.54	18	60	2.45	1.5	7	278	68	1.58	300	0.23	1.15	47	12	42	1650	6	2.4	2	88	5	80	5	176	
SP-157	200	230	S.C. 30'	7	0.8	0.92	6	370	5.1	1	6	172	54	1.58	180	0.28	2.07	29	12	37	1800	14	3	3	104	5	95	5	172	
SP-157	230	300	RHs 70'	37	0.4	0.49	38	870	8.98	0.5	3	73	35	0.89	190	0.22	0.536	29	5	18	760	4	2.4	2	115	5	31	5	72	
SP-157	300	350	RHs 50'	103	0.8	0.72	60	380	8.08	1	3	62	22	1.07	630	0.35	0.45	20	4	24	1270	6	2.8	2	93	5	70	5	106	
SP-157	350	400	RHs 50'	75	0.8	0.74	104	300	7.92	1	2	56	17	0.89	780	0.27	0.484	19	2	14	1020	4	3.2	2	78	5	40	5	82	
SP-157	400	450	RHs 50'	184	0.2	0.54	38	320	8.51	2.5	3	56	17	0.89	780	0.38	0.488	14	3	22	2120	6	3.4	2	94	5	107	5	142	
SP-157	450	500	RHs 50'	184	0.2	0.54	50	140	7.94	1.3	2	73	18	0.89	1750	0.27	0.484	14	3	21	1900	4	4	2	84	5	53	5	112	
SP-157	500	525	RHs 25'	370	0.8	0.32	78	350	7.44	1	1	159	14	0.67	5250	0.14	0.53	14	6	18	1070	4	5.4	1	65	5	50	5	72	
SP-157	525	545	H.C. 2.3 20'	263	0.1	0.21	68	800	15	0.25	1	503	12	0.48	8200	0.03	0.09	3	13	16	480	2	4.2	0	6	5	11	5	32	
SP-157	545	600	H.C. 2.3 50'	263	0.1	0.21	68	800	15	0.25	1	15	8	0.58	3050	0.12	0.69	21	0	4	260	2	4.2	1	395	5	7	5	18	
SP-157	600	650	H.C. 3 50'	9	0.1	0.5	28	180	13	0.25	2	9	9	0.74	410	0.3	1.52	22	0	6	200	2	0.8	1	1120	40	5	5	28	
SP-157	650	700	H.C. 3 50'	3	0.1	0.28	14	60	15	0.25	2	9	6	0.56	100	0.19														



Appendix 1:  
SSX Geochemical Data For Surface Drill Holes Intercepting Mapped Workings

SP-265	FROM	TO	Lithology	Au (ppb)	Ag (ppm)	Al %	As (ppm)	Ba (ppm)	Ca %	Cd (ppm)	Cu (ppm)	Cr (ppm)	Cu (ppm)	Fe %	Hg (ppb)	K %	Mn %	Mo (ppm)	Na (ppm)	P (ppm)	Pb (ppm)	Sb (ppm)	Sc (ppm)	Sr (ppm)	Ti (ppm)	V (ppm)	W (ppm)	Zn (ppm)		
SP-265	0	50 S.C. 50'		13	0.1	0.79	14	270	1.55	1.5	7	51	83	1.69	360	0.38	0.78	28	12	42	1490	8	5.4	2	68	5	97	5	184	
SP-265	50	100 S.C. 50'		8	0.4	0.95	12	200	2.98	0.5	7	122	51	1.7	180	0.34	1.53	22	7	37	1110	6	2.4	3	69	5	40	5	142	
SP-265	100	150 S.C. 20'		7	0.1	0.78	8	190	4.57	1.3	6	118	63	1.8	200	0.38	2.07	19	12	44	2180	4	3.6	3	104	5	80	5	220	
SP-265	120	150 R.H.s. 30'		3	0.1	0.82	8	550	8.69	3.3	5	53	54	1.41	300	0.35	4.05	16	26	69	2180	8	5.2	3	203	5	121	5	310	
SP-265	150	200 R.H.s. 50'		3	0.1	0.53	18	670	7.86	4.5	2	48	61	0.88	400	0.25	5.25	10	41	85	3920	6	5.0	3	242	5	223	5	342	
SP-265	450	500 R.H.s. 50'		25	0.1	0.49	52	510	12.4	0.5	1	39	15	0.84	260	0.27	4.31	21	21	19	890	6	1.8	2	91	5	28	5	90	
SP-265	500	540 R.H.s. 40'		7	0.2	0.6	52	420	7.54	1	10	42	26	1.49	280	0.27	4.14	28	1	38	870	4	1.8	6	83	5	29	5	84	
SP-265	540	595 R.H.s. 25'		28	0.2	0.43	38	660	8.27	1	2	38	14	0.78	840	0.21	4.75	24	1	18	770	6	2.2	2	75	5	45	5	92	
SP-265	595	570 Dike 5'		32	0.8	0.52	64	280	9.53	4	7	31	28	1.3	410	0.28	5.45	21	5	48	1980	6	2.4	4	98	5	152	5	204	
SP-265	570	500 R.H.s. 20'		71	0.4	0.42	46	920	9.02	2	3	32	17	0.95	2650	0.23	5.06	23	1	24	1810	2	2.8	2	83	5	78	5	152	
SP-265	650	650 Fault in H.C. 60'		1350	1.2	0.15	298	410	9.27	0.5	2	78	13	0.82	16900	0.1	2.14	14	3	12	560	2	9.4	1	182	5	12	5	50	
SP-265	650	750 H.C. 3. 50'		2800	0.1	0.17	480	410	15	0.25	3	3	11	0.68	18500	0.17	1.33	20	0	6	230	1	1.8	1	819	5	3	5	46	
SP-265	750	800 Fault in H.C. 50'		10000	0.1	0.42	5530	110	15	0.5	13	24	45	2.19	99000	0.28	1.04	29	0	38	550	1	2.4	1	819	5	3	5	42	
SP-265	800	850 H.C. 3. 4. 50'		1800	0.1	0.25	368	220	13.55	0.25	3	43	11	0.75	12800	0.17	2.03	19	2	10	1350	1	13.3	6	346	5	14	10	54	
SP-265	850	900 H.C. 4. 50'		1450	0.1	0.1	288	870	15	0.25	2	22	6	0.4	9160	0.08	2.01	8	0	7	2210	1	3.8	0	337	5	6	5	36	
SP-265	900	950 H.C. 4. 50'		59	0.1	0.09	48	250	15	0.25	1	15	4	0.41	2050	0.07	1.74	10	0	5	1320	1	7.4	0	592	5	3	5	34	
SP-265	950	1000 H.C. 4. 50'		105	0.1	0.04	60	110	15	0.25	0.5	37	3	0.3	2520	0.03	1.86	18	1	3	830	1	120	0	225	5	4	5	28	
SP-243	FROM	TO	Lithology	Au (ppb)	Ag (ppm)	Al %	As (ppm)	Ba (ppm)	Ca %	Cd (ppm)	Cu (ppm)	Cr (ppm)	Cu (ppm)	Fe %	Hg (ppb)	K %	Mn %	Mo (ppm)	Na (ppm)	P (ppm)	Pb (ppm)	Sb (ppm)	Sc (ppm)	Sr (ppm)	Ti (ppm)	V (ppm)	W (ppm)	Zn (ppm)		
SP-243	20	50 S.C. 30'		13	0.2	0.92	36	70	1.66	0.25	9	68	85	1.69	300	0.27	0.96	50	7	38	770	8	2.4	3	68	5	35	5	108	
SP-243	50	100 S.C. 50'		6	0.0	0.56	40	90	2.74	1	9	73	62	1.53	230	0.26	1.51	32	7	39	1110	8	2.0	3	70	5	44	5	172	
SP-243	100	155 S.C. 55'		13	0.4	0.81	106	60	2.74	1	5	10	89	75	2.04	370	0.27	1.38	25	9	48	1830	8	2.4	3	81	5	54	5	188
SP-243	155	200 R.H.s. 50'		3	0.4	0.35	30	410	10.1	1.5	4	35	47	0.95	330	0.17	1.54	15	22	58	2270	6	3.2	3	159	5	85	5	188	
SP-243	200	250 R.H.s. 50'		2	0.1	0.37	28	350	8.52	1	3	32	28	0.89	160	0.17	4.31	17	3	32	1210	4	2.8	3	108	5	49	5	114	
SP-243	250	300 R.H.s. 50'		18	0.1	0.39	20	820	7.57	0.5	3	28	20	0.93	120	0.17	4.31	17	3	24	810	4	1.4	2	89	5	20	5	87	
SP-243	300	350 R.H.s. 50'		28	0.4	0.35	60	540	9.94	4	2	31	40	1.03	310	0.16	5.94	36	22	66	2540	4	6.4	2	104	5	249	5	426	
SP-243	350	400 R.H.s. 50'		4	2	0.25	60	200	10.55	11.5	2	41	84	0.88	890	0.11	6.69	16	83	154	890	6	17	3	121	5	274	5	1150	
SP-243	400	425 R.H.s. 25'		25	0.2	0.29	94	120	7.89	5	2	37	44	0.95	830	0.12	4.87	35	22	64	1340	6	7.6	2	80	5	890	5	496	
SP-243	425	500 H.C. 2.3. 25'		338	0.1	0.12	210	540	13.8	0.25	1	10	10	0.78	2200	0.07	6.54	24	4	7	330	2	7.4	1	210	5	274	5	34	
SP-243	500	550 H.C. 3. 50'		4	0.2	0.18	138	560	15	0.25	3	5	9	0.79	280	0.12	0.92	21	0	8	220	2	0.8	1	572	5	4	5	30	
SP-243	550	600 H.C. 3. 50'		0	0.1	0.18	42	170	15	0.25	2	3	7	0.52	250	0.12	1.25	19	0	4	180	1	0.1	1	1050	5	3	5	20	
SP-243	600	650 H.C. 3. 50'		0	0.1	0.25	14	140	15	0.25	2	3	9	0.61	60	0.17	1.38	22	0	5	220	1	0.1	1	1185	5	3	5	24	
SP-243	650	700 H.C. 3. 50'		12	0.1	0.18	36	260	15	0.25	2	4	9	0.59	330	0.13	1.39	21	0	5	210	1	0.1	1	978	5	2	5	20	
SP-243	700	740 H.C. 3. 50'		18	0.1	0.13	24	110	15	0.25	2	3	7	0.4	210	0.09	1.19	17	0	4	220	1	0.2	1	1140	5	2	5	18	
SP-243	815	850 H.C. 4. 35'		99	0.1	0.04	2540	200	15	0.25	0.5	12	6	0.09	3650	0.02	1.1	4	1	4	1860	1	21	0	281	5	2	5	18	
SP-243	850	900 H.C. 4. 50'		6	0.1	0.13	18	80	15	0.25	0.5	9	7	0.16	150	0.07	1.3	3	2	3	1360	1	0.2	0	586	5	2	5	20	
SP-243	900	925 H.C. 4. 25'		3	0.1	0.19	20	120	15	0.25	0.5	10	8	0.33	120	0.11	1.37	5	0	4	1430	4	0.2	0	758	5	3	5	22	
SP-339C	FROM	TO	Lithology	Au (ppb)	Ag (ppm)	Al %	As (ppm)	Ba (ppm)	Ca %	Cd (ppm)	Cu (ppm)	Cr (ppm)	Cu (ppm)	Fe %	Hg (ppb)	K %	Mn %	Mo (ppm)	Na (ppm)	P (ppm)	Pb (ppm)	Sb (ppm)	Sc (ppm)	Sr (ppm)	Ti (ppm)	V (ppm)	W (ppm)	Zn (ppm)		
SP-339C	10	55 S.C. 45'		6	0.0	0.93	30	140	2.91	1.5	6	237	56	1.54	200	0.39	1.41	24	7	33	1920	6	3.4	3	89	5	60	5	142	
SP-339C	55	100 R.H.s. 45'		1	0.4	0.52	18	600	9.72	2.5	4	50	50	1.19	360	0.24	5.73	25	28	82	2070	6	3.0	3	149	5	113	5	190	
SP-339C	100	150 R.H.s. 50'		0	0.0	0.59	14	640	10.5	2	3	51	45	0.94	390	0.25	5.21	14	22	55	2810	4	3.4	3	188	5	122	5	196	
SP-339C	150	200 R.H.s. 50'		0	0.1	0.91	8	720	8.26	0.5	3	46	18	1	60	0.25	5.37	23	3	18	410	10	2.1	3	104	5	21	5	46	
SP-339C	200	250 R.H.s. 50'		11	0.1	0.83	20	780	8.48	2	3	48	25	1.15	160	0.47	5.48	21	4	22	950	8	2.4	3	106	5	78	5	124	
SP-339C	250	300 R.H.s. 50'		4	0.8	0.91	20	440	9.08	4	3	49	45	1.12	400	0.33	5.7	23	20	58	2280	6	6.4	3	132	5	189	5	268	
SP-339C	300	350 Fault in R.H.s. 50'		13	0.2	0.8	24	240	8.89	1	3	53	30	1.09	280	0.34	5.21	16	5	31	1360	6	2	3	115	5	52	5	108	
SP-339C	350	400 R.H.s. 50'		21	0.1	0.48	42	280	7.47	1	3	44	18	0.9	480	0.38	5.54	21	3	18	390	6	1.8	2	89	5	23	5	60	
SP-339C	400	450 R.H.s. 50'		36	0.2	0.99	80	380	8.22	1	3	44	22	1.08	620	0.25	3.65	13	1	14	930	4	1.4	2	121	5	49	5	98	
SP-339C	450	500 R.H.s. 50'		19	0.4	0.51	28	310	11.25	0.5	2	28	18	0.68	820	0.25	3.65	13	1	14	930	4	1.4	2	121	5	49	5	98	
SP-339C	500	540 R.H.s. 40'		55	0.4	0.93	44	510	8.31	0.5	2	42	18	0.79	1020	0.3	4.33	14	2	19	1370	4	1.8	2	78	5	45	5	70	
SP-339C	540	545 H.C. 1000 5'		0	0.1	0.27	14	230	15	0.25	2	42	12	0.55	50	0.21	1.47	21	0	4	170	2	0.1	1	1445	5	3	5	18	
SP-339C	545	600 Fault in H.C. 95'		150	0.1	0.18	80	370	14	0.1	0.5	239	11	0.5	1400	0.08	0.65	4	8	16	860	1	2.8	0	15	5	27	5	50	
SP-339C	600	650 H.C. 3. 50'		610	0.1	0.26	214	400	14.6	0.25	2	25	12	0.71	3310	0.18	4.5	20	1	7	330	2	6.8	0	399					